

Technical report

# The materials and the design of the die in a critical manufacturing step of an automotive shock absorber cap

G.C.R. Moura <sup>a</sup>, M.T.P. Aguilar <sup>b</sup>, A.E.M. Pertence <sup>c</sup>, P.R. Cetlin <sup>a,\*</sup>

<sup>a</sup> Department of Metallurgical and Materials Engineering, Federal University of Minas Gerais, Engineering School, Rua Espírito Santo 35, Belo Horizonte, Minas Gerais 31160-030, Brazil

<sup>b</sup> Department of Construction and Materials, Federal University of Minas Gerais, Engineering School, Rua Espírito Santo 35, Belo Horizonte, MinasGerais 31160-030, Brazil

<sup>c</sup> Department of Mechanical Engineering, Federal University of Minas Gerais, Engineering School, Rua Espírito Santo 35, Belo Horizonte, MinasGerais 31160-030, Brazil

Received 8 April 2005; accepted 18 October 2005  
Available online 29 November 2005

## Abstract

The industrial drawing of automotive shock absorber endcaps caused wear and radial brittle fractures of the tool steel dies. A finite element method (FEM) simulation of the process showed that this was caused by high contact and hoop stresses on the die. Such difficulties are usually solved by expensive changes in the die material, but a change in the punch design was proposed as a simpler and cheaper solution. The new punch geometries were employed in a FEM simulation of the drawing, indicating much lower contact and hoop stresses. The implementation of the solution eliminated the wear and brittle fracture problems.

© 2005 Elsevier Ltd. All rights reserved.

## 1. Introduction

Fig. 1 illustrates a typical tubular car shock absorber [1]. The endcap (1) is welded to the tubular body (2) and to the fastening ring (3) of the shock absorber. This ring is screwed to the car body, allowing the shock absorber to actuate during the oscillations and impacts undergone by the car wheels.

The end cap is manufactured through deep drawing, involving the pressing of a punch on a circular blank located over a cylindrical die, as illustrated in Fig. 2. The figure also shows the blank holder, on which a constant load of 1.0 kN is applied. The feeding of blanks to the press is performed manually.

The blank material is an AISI 1008 carbon steel, 26.7 mm in radius and 2.75 mm thick. The die, punch and blank holder are made out of a conventional D3 tool

steel (2.0%C, 11.50%Cr, 0.30%Mn, 0.2%V, hardness in the range of 56–64 HRC, as quenched and tempered).

After a relatively small number of pressings (about 200), a premature wear in the die throat, in the region indicated in Fig. 2, was observed. This resulted in an unacceptable scratching of the external lateral surface of the endcap and led to frequent production problems, involving the replacement and repolishing of the dies. Fig. 3 displays the external surface of a scratched endcap, viewed with a scanning electron microscope (SEM), under a 15 kV voltage. The specimen underwent a preliminary ultrasonic cleaning in acetone. Another problem was the occasional radial cracking of the die during the processing, illustrated in Fig. 4.

The objective of the present paper was to analyze the drawing of the endcap and propose changes in the design of the dies, so that the usual materials employed for such dies (tool steels) could be used without the wear and cracking problems. This analysis involved a finite element simulation of the die manufacturing, allowing the evaluation of the stresses on the die in this manufacturing step.

\* Corresponding author. Tel.: +55 31 3238 1849; fax: +55 31 3238 1815.  
E-mail address: [p cetlin@demet.ufmg.br](mailto:p cetlin@demet.ufmg.br) (P.R. Cetlin).

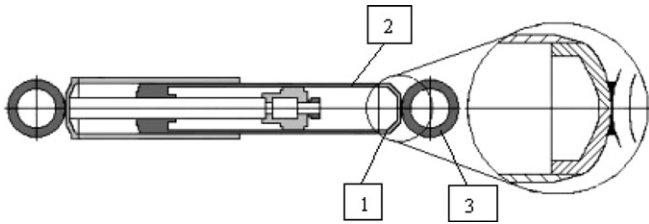


Fig. 1. An automotive shock absorber and a detail of the endcap.

**2. Method**

*2.1. Numerical simulation through the finite element method*

*2.1.1. Parameters in the simulation*

The forming under discussion was simulated utilizing the finite element method, employing the commercial software DEFORM® 7.0 for Windows (Scientific Forming Technologies Corporation, OH (USA)). The process was considered as axisymmetric, and Fig. 5 illustrates the drawing utilized for the simulation. Parts 3 and 4 in Fig. 5 were taken as rigid (no elastic deformation). Since it was necessary to evaluate the stress levels in part 1, it was considered as elastic, with a Young’s modulus of 202 GPa

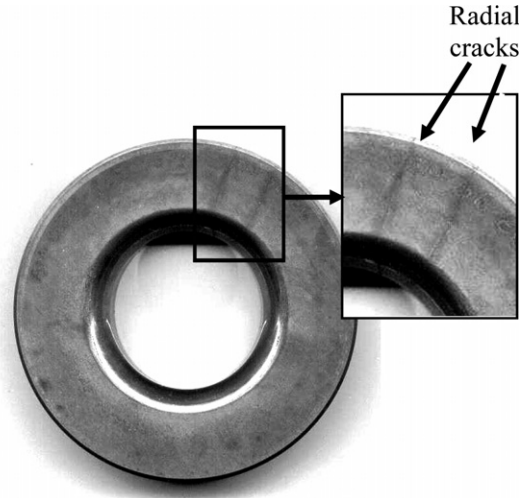


Fig. 4. Radial cracks in the drawing die.

and a Poisson coefficient  $\nu = 0.3$ . For the simulation, the finite element mesh of this part had 3500 quadratic elements. This simulation was called CA-0-1.

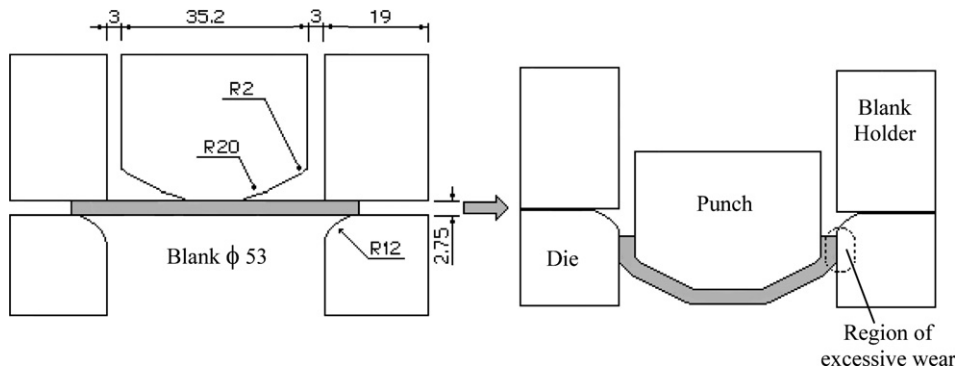


Fig. 2. Schematic illustration of the endcap manufacturing process (dimensions in mm).

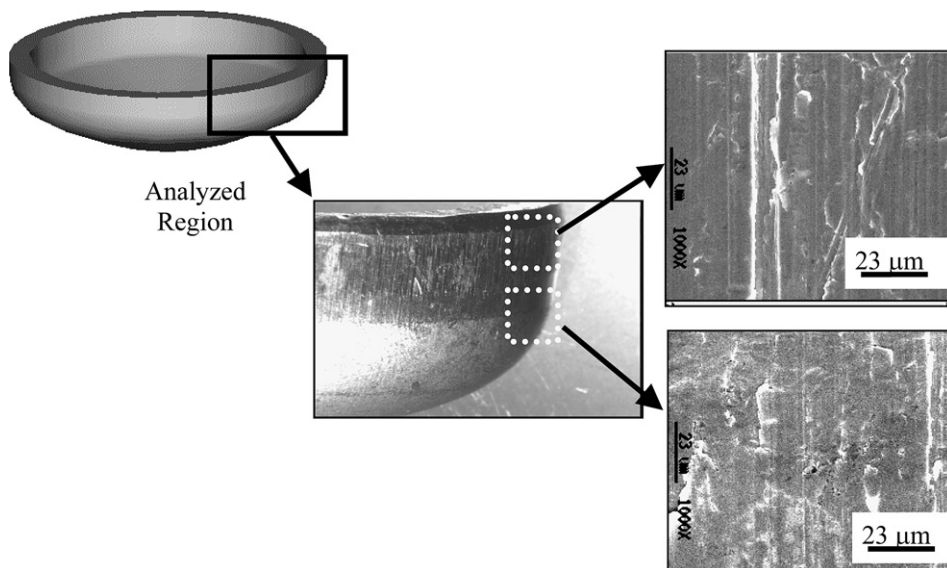


Fig. 3. Lateral surface of a scratched endcap (SEM).

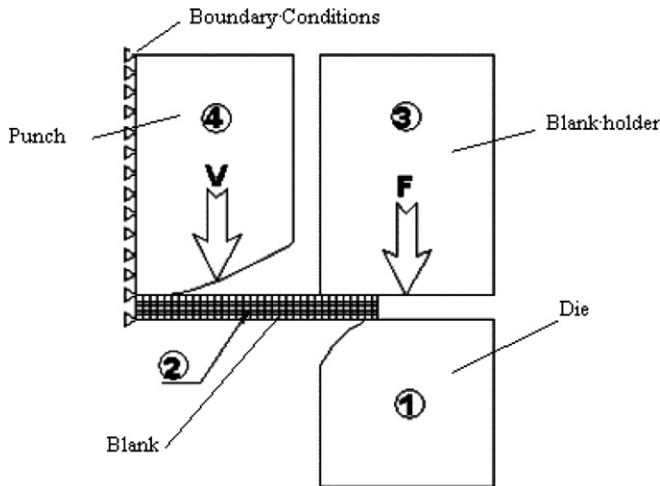


Fig. 5. Illustration of the processing geometry utilized in the FEM simulation of the endcap processing.

Several finite element meshes were considered for the blank (part 2, Fig. 5), in order to speed the computing time and increase the precision of the results. An insufficient number of elements may cause instabilities in the calculated loads on the dies during the simulation. A mesh of 3000 elements was thus employed, causing load oscillations on the tools of about 8% of the maximum observed loads. The computer time for such a mesh was about 5 times that for a mesh with 500 elements, which, on the other hand, caused load oscillations of up to 45% of the maximum observed loads. The blank mesh included regions with different densities of elements, allowing the use of a higher number of elements in the regions subject to more severe strains, close to the outer borders of the blank. The element density in this region was 5 times that in the central region, as illustrated in Fig. 6.

The die did not move during the simulation. The punch vertical speed was  $V = 10$  mm/s, and the load on the blank holder was  $F = 1.0$  kN. The material of the blank was considered as rigid-plastic, and its stress-strain curve was the one in the internal library of DEFORM® for the AISI 1008 steel at room temperature. The time for the movement of the punch in each step of the simulation was 0.10 s, and the simulation was run for 225 steps.

2.1.1. Validation of the FEM simulation

The finite element simulation was validated through a comparison of the predicted and experimental thickness of the endcap at different points along its profile. Fig. 7 shows the points in the endcap, where the thicknesses were measured. The horizontal distance between points 1 and 9 was 2 mm and the vertical distance between points 10 and 12 was also 2 mm. Experimental measurements were performed in a longitudinal section of the endcap and utilized a Mitutoyo PJ311 shadowgraph, under a magnification of 20x and digital micrometers allowing a 1/1000 mm precision. Measurements in the numerical simulation employed the virtual measuring system of DEFORM.



Fig. 6. Finite element mesh employed for the blank.

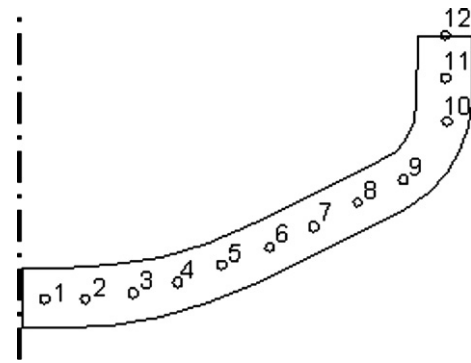


Fig. 7. Points in the endcap for thickness measurements.

Fig. 8 shows the experimental and numerical values for the thickness measured at the points shown in Fig. 7. The agreement is quite reasonable, which is an indication that the present finite element method (FEM) simulation represents fairly well the real processing. An important point is that a thickening of the endcap, in relation to its initial thickness, is predicted (and experimentally observed) in its outer region (points 9–12).

Fig. 9 shows a sequence of the simulated drawing operation, starting in step 120 and up to step 220. The thickening of the outer region of the blank can be clearly identified, from step 160 to 185. This thicker region then undergoes an ironing operation, starting approximately at step 190 and ending around step 210. Both the thickening and the ironing are indicated in Fig. 9.

2.2. Pressure on the die

Fig. 10 shows the variation of the maximum radial pressure ( $\sigma_x$ ) of the material on the die, predicted by the numerical simulation, and that occurred in the region indicated in Fig. 2. It is during the ironing phase of the forming (illustrated in Fig. 9) that one can observe a substantial increase in the contact pressure, which reaches a peak of 920 MPa in step number 210.

Fig. 11 shows a comparison of the adhesive wear behavior [2–4] (utilizing Archard's constant  $-k_A$ ) of various materials under increasing contact pressure [7]. The vertical line "A" corresponds to the maximum contact pressure (920 MPa – see Fig. 10) predicted in the numerical simulation CA-0-1. It can be seen that tool steels working under such conditions will present excessive levels of wear. The solution would involve ceramic inserts at the high pressure locations or the adoption of surface coatings such as TiN, both of which are more wear resistant than tool steels. Both

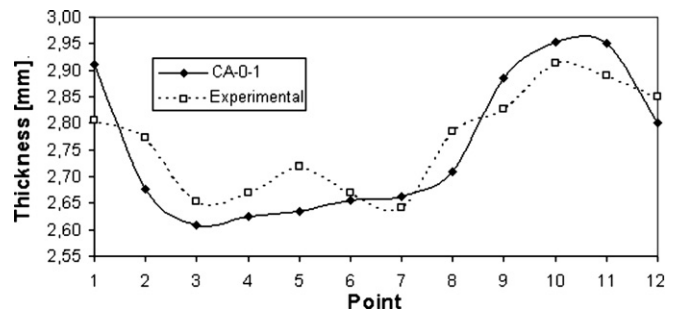


Fig. 8. Experimental and numerical thickness of the endcap at the points indicated in Fig. 7.

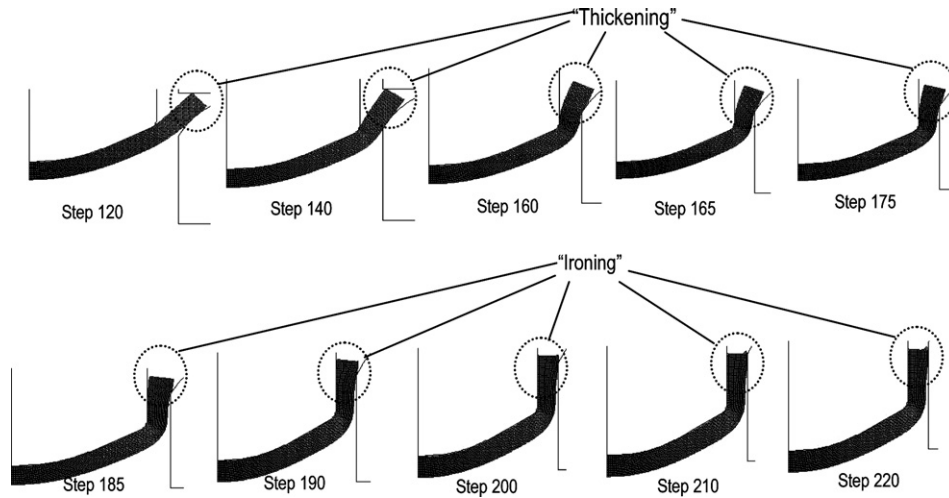


Fig. 9. Thickening and ironing in the numerical simulation of the drawing of the endcap.

solutions are technologically complex and involve additional costs. A simpler and cheaper solution would be a change in the die design in order to decrease the contact pressure.

2.3. Fracture stresses on the die

The cracks illustrated in Fig. 3 are caused by the tensile hoop stresses ( $\sigma_y$ ) on the die during the drawing operation. The numerical simulations revealed that these stresses occur at the internal diameter of the die throat. Fig. 12 shows the evolution of  $\sigma_y$  during the drawing of the endcap. Similarly to what was shown in Fig. 10 for the contact pressure, the ironing phase leads to a maximum in the hoop stresses, reaching a value of 681 MPa in step number 210.

The fracture toughness ( $K_{IC}$ ) of tool steels ranges from 20 to 30 MN m<sup>-3/2</sup> [7]. Considering the above mentioned maximum value of the hoop stress ( $\sigma_y = 681$  MPa) one can calculate the approximate ranges of the larger superficial crack that the die material will tolerate without catastrophic brittle fracture, through the following equation

$$K_{IC} = \sigma_y \sqrt{\pi c}, \tag{1}$$

where  $c$  is the depth of the superficial crack. The critical depth is 0.27 mm for  $K_{IC} = 20$  MN m<sup>-3/2</sup> and 0.62 mm for  $K_{IC} = 25$  MN m<sup>-3/2</sup>. The calculations were performed without any safety margin, and it is perfectly pos-

sible that such cracks may already be in the material as a result of the manufacturing steps (machining and heat treatment) or are originated by the stress concentrations associated with the roughening of the surface caused by the surface scratching shown in Fig. 3.

In the present situation, ceramic, wear resistant inserts could be adopted only if such inserts were interference mounted in the die. Ceramics have very low fracture toughness, and would easily crack radially under the applied hoop stresses. This is another indication of the convenience of die design changes in order to lower the prevailing stresses during the drawing operation.

2.4. Proposed changes in the die set design

The analysis of the evolution of the contact and hoop stresses in the die reveals that these stresses reach critical values only during the ironing of the material between the punch and the die itself during the drawing operation. Changes in the die geometry cannot be adopted, since the die throat defines the external diameter of the endcap, which must fit into the internal diameter of the shock tube (see Fig. 1). On the other hand, changes in the punch geometry can be considered, in case they lead to a decrease of the ironing intensity and do not lead to changes in the external diameter of the endcap. Fig. 13 shows two punch design options which were analyzed in the present paper (called simulations CA-0-2 and CA-0-3, respectively), in order to decrease the ironing stresses in the die. The results of the FEM simulation for these three situations are shown in Fig. 14, clearly indicating the lower levels of ironing associated with simulations CA-0-2 and CA-0-3, in comparison with simulation CA-0-1.

3. Results and discussion

3.1. Effect of the punch geometry changes on the endcap wall thickness

Fig. 15 shows the values predicted by the FEM simulation for the endcap wall thickness for the 3 punch geometries under discussion. The experimental and numerical thicknesses were evaluated at the same points already discussed in connection with Fig. 7, and the experimental results for the CA-0-1 design are those in Fig. 8.

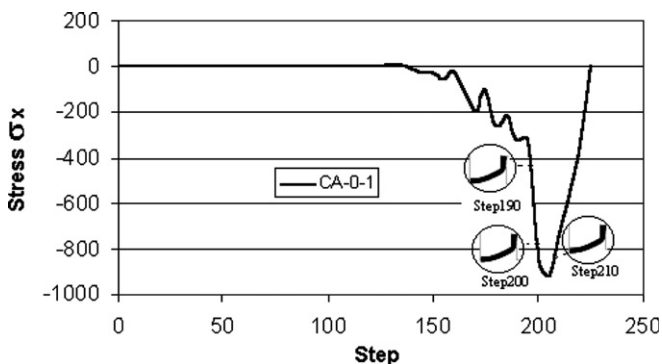


Fig. 10. Maximum radial pressure of the material on the die in the CA-0-1 simulation.

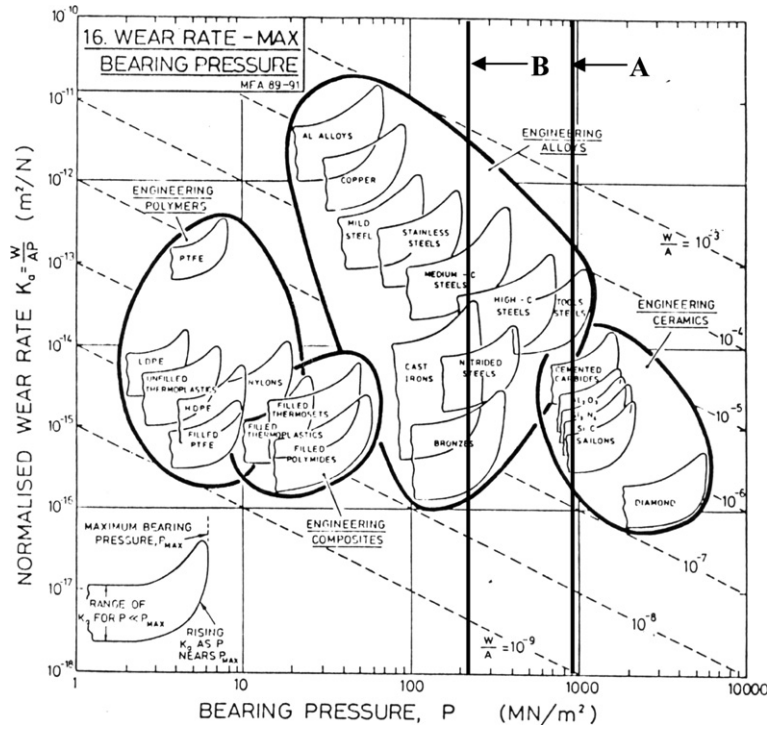


Fig. 11. The wear of materials under increasing contact pressures [7].

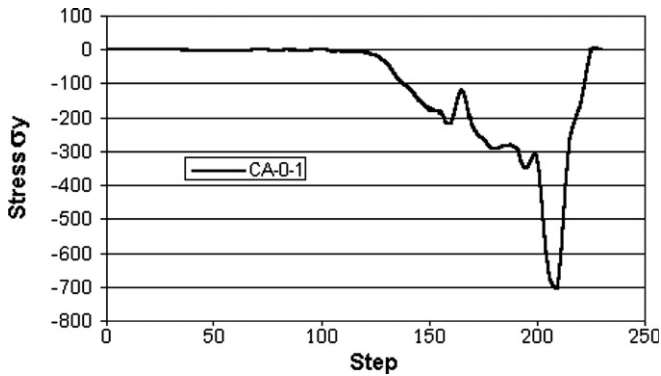


Fig. 12. The evolution of the maximum hoop stress ( $\sigma_y$ ) in the die during the drawing.

Simulations CA-0-2 and CA-0-3 lead to a higher wall thickness at the central and border regions of the endcap. These changes, however, are quite low (an increase of a maximum of 0.1 mm in relation to simulation CA-0-1). In addition, no changes in the external diameter of the endcap were observed, and no difficulties should be observed in the assembling and welding of the endcap to the tube.

3.2. The effect of the punch design changes in the contact pressure between the material and the die

Fig. 16 shows the variation of the maximum radial pressure ( $\sigma_x$ ) of the material on the die, predicted by the numerical simulation, for the three punch geometries under

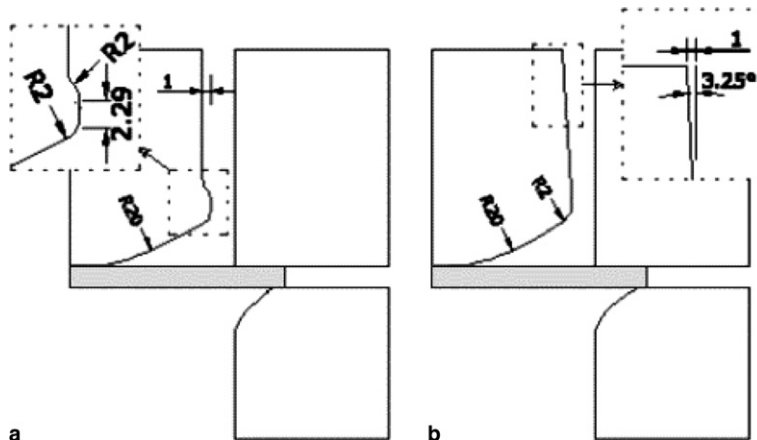


Fig. 13. Proposed changes in the punch design: CA-0-2 (a) and CA-0-3 (b).

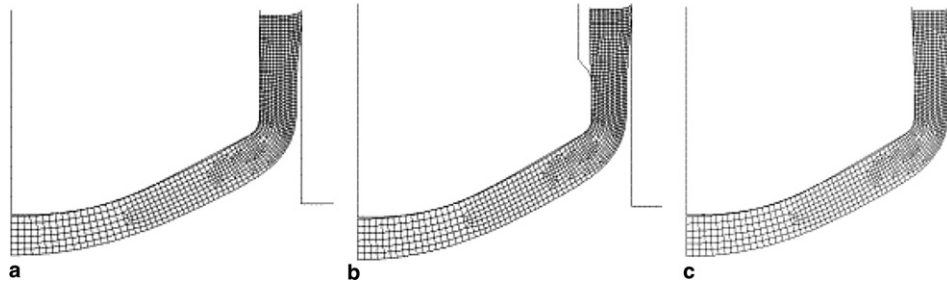


Fig. 14. Ironing degree at the last step of the FEM simulation (step number 225) for simulations: CA-0-1 (a), CA-0-2 (b) and CA-0-3 (c).

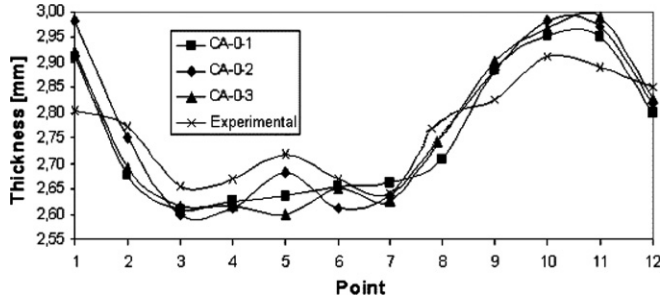


Fig. 15. Comparison of the numerically predicted wall thickness of the endcap for the 3 punch designs with the experimental thickness for punch CA-0-1.

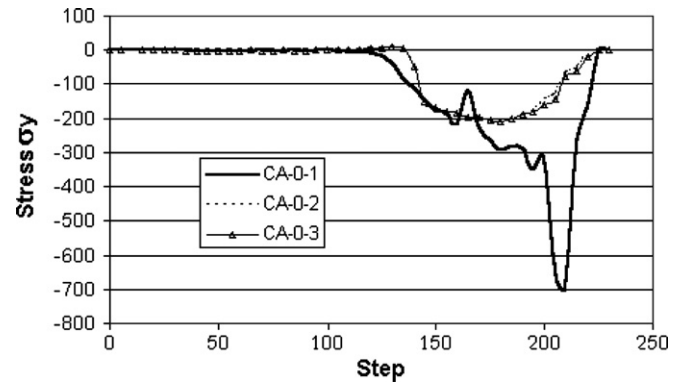


Fig. 17. The evolution of the maximum hoop stress ( $\sigma_y$ ) on the die for the three punch geometries under consideration.

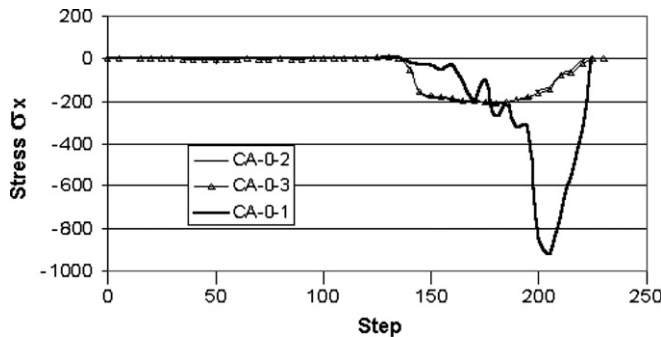


Fig. 16. Numerically predicted contact stress between the material and the die ( $\sigma_x$ ) for the three punch geometries under consideration.

consideration. There was a decrease in the maximum pressure from a value of 920 MPa for simulation CA-0-1, to about 200 MPa, for simulations CA-0-2 and CA-0-3. This level of pressure is indicated in Fig. 11 by line B, corresponding to a much better wear performance of the tool steel dies. This was the case when both punch geometries were industrially tested. The figure suggests that an even cheaper material, such as a high Carbon steel, could be considered for the die material, from the point of view of die wear.

### 3.3. The effect of the punch design changes on the fracture stress on the die

Fig. 17 shows the results for the evolution of the maximum hoop stress on the die ( $\sigma_y$ ) for the three punch geom-

etries under consideration. There was a decrease from a maximum value of  $\sigma_y = 681$  MPa in simulation CA-0-1, to a value of  $\sigma_y$  of  $\approx 190$  MPa for simulations CA-0-2 e CA-0-3.

If one now considers the maximum value of the hoop stress as  $\sigma_y = 190$  MPa, the critical depth of a superficial crack leading to brittle fracture would be 3.53 mm for  $K_{IC} = 20 \text{ MN m}^{-3/2}$  and 7.93 mm for  $K_{IC} = 30 \text{ MN m}^{-3/2}$ . These values for the critical crack depth are much higher than those previously calculated for the punch geometry CA-0-1, involving a very remote possibility of brittle fracture of the die. No such fractures were indeed observed under industrial practice.

## 4. Conclusions

The numerical finite element simulations of the drawing of a shock absorber endcap, employing the DEFORM<sup>®</sup> software, supplied results close to those from the real industrial processing. This was validated through the dimensional similarity between the real part and the simulated one.

The wear failure in the drawing die throat is caused by the high contact pressures associated with the ironing of the material between the punch and the die during the final drawing stage. The ironing also causes high tensile hoop stresses in the die, which thus suffers occasional brittle radial fractures.

The above wear and fracture problems were eliminated through a change in the punch geometry, which decreased the contact and hoop stresses associated with the ironing stage. The punch design change is much simpler and cheaper than the adoption of ceramic inserts or hard surface layers on the die.

#### **Acknowledgements**

The authors are grateful for the financial support of PRONEX-MCT, CNPq-MCT and CAPES-MEC.

#### **References**

- [1] Basso R, Fanti G. In: Proceedings of the first international conference on the integration of dynamics, monitoring and control (DYMAC 99), Manchester (United Kingdom); September 1–3, 1999.
- [2] Wulpi DJ. Understanding how components fail. 1st ed. Metals Park (OH, USA): American Society for Metals; 1985 [p. 163, chapter 11].
- [3] Dieter GE, editor. (Materials selection and design), design for wear resistance. Metals handbook, vol. 20. Materials Park (OH, USA): ASM International; 1997. p. 603.
- [4] Ashby MF. Materials selection in mechanical design. 1st ed. Oxford: Pergamon Press; 1992. p. 22, 53.
- [5] CES 4.1 EduPack Software. Granta Corporation; 2003.